RESEARCH PAPER

A Novel Quinoxaline Derivatives Targeting Estrogen Receptor in Breast Cancer: Design, Molecular Docking and Md Simulations

Abitha H[1,2], D. Kumudha[1*]

[1]Faculty of Pharmacy, Karpagam Academy of Higher Education, Coimbatore-641021, Tamil Nadu, India
[2]Department of Pharmaceutical Chemistry, Nehru College of Pharmacy, Thrissur-680588, Kerala, India.

E-mail: deanfop@kahedu.edu.in, abithaharidas8@gmail.com

ABSTRACT

Estrogen receptor α (ERα) is a key therapeutic target in estrogen receptor–positive breast cancer. In this study, nine phenoxy quinoxaline derivatives (QP1–QP9) were designed and evaluated as potential ERα antagonists using molecular docking and molecular dynamics simulations. Docking studies were performed with the crystal structure PDB 6WOK using Glide–Schrödinger, with tamoxifen as the reference ligand. The compounds exhibited binding affinities ranging from −8.480 to −10.974 kcal/mol, surpassing tamoxifen (−9.126 kcal/mol). Compounds QP8 and QP9 showed favourable interactions, including hydrogen bonding with TYR87 and GLN100 and hydrophobic and π-stacking contacts with PHE98 and TYR36/55. Docking reliability was confirmed through redocking of the co-crystallized ligand. SwissADME and pkCSM analyses indicated good drug-likeness, high gastrointestinal absorption, and acceptable ADMET profiles, though potential CYP450 inhibition requires further study. A 100 ns molecular dynamics simulation of the QP8–ERα complex demonstrated structural stability, supporting QP8 as a promising lead for further experimental validation.

Keywords: Phenoxy quinoxaline derivatives; Estrogen receptor α (ERα); Molecular docking; Drug-likeness; ADMET prediction; Molecular dynamics simulation; Breast cancer; In silico drug design.

How to cite this article: Abitha H, Kumudha D. A Novel Quinoxaline Derivatives Targeting Estrogen Receptor in Breast Cancer: Design, Molecular Docking and Md Simulations. Int J Drug Deliv Technol. 2026;16(37s): 529-538. DOI: 10.25258/ijddt.16.37s.70

Source of support: Nil

Conflict of interest: None

1. INTRODUCTION

Approximately one in eight women in the United States may develop breast cancer at some point in their lives, making it the most common cancer diagnosed in women globally. In addition to 59,080 new cases of non-invasive breast cancer known as ductal carcinoma in situ (DCIS), approximately 316,950 women and 2,800 men in the United States are expected to receive a diagnosis of invasive breast cancer in 2025. Despite its prevalence, breast cancer survival rates have significantly increased due to early detection, improved screening, and therapeutic advancements, reaching a 5-year relative survival rate of 99% for localized cases (1-2).

Genetic changes that cause unchecked proliferation and tumorigenesis in healthy breast cells give rise to breast cancer. These mutations could be caused by a combination of environmental, hormonal, and genetic factors that disrupt normal cell cycle regulation. Over time, some breast cells proliferate abnormally to form a lump or tumor that, if untreated, may spread to other parts of the body or infiltrate nearby tissues.

The process frequently starts in the breast's lobules (lobular carcinoma) or ducts (ductal carcinoma). While advanced breast cancer spreads through the lymphatic and circulatory systems and infiltrates nearby tissues, early-stage breast cancer is frequently contained within ducts or lobules. Breast cancer risk is significantly increased by genetic mutations in tumor suppressor genes (BRCA1, BRCA2) or oncogenes (HER2). Hormonal factors, such as extended exposure to estrogen, also affect the growth of tumors.

The annual incidence and death rates of breast cancer are approximately 130.8 per 100,000 women and 19.2 per 100,000 women, respectively. It is estimated that 42,170 women in the US will die from breast cancer in 2025. Because of screening and early detection, age-related increases in risk have led to higher survival rates (3-5).

In 2022, there were over 2.3 million new cases of breast cancer reported globally, and in many countries, the incidence is increasing at a rate of 1–5% annually. Mortality rates vary by region and sharply decrease in countries with a high Human Development Index (HDI) as a result of better access to healthcare. Risk factors

include age, family history, genetic mutations, exposure to hormones, obesity, alcohol consumption, and lifestyle choices. Early diagnosis, improved treatments, and preventative measures are critical to managing the burden of disease worldwide (6-7).

Researchers are constantly looking for effective targets to improve therapeutic approaches because breast carcinoma is one of the most prevalent and deadly types of malignancies. Molecular and histological kinds of breast cancer can be used to categorize the disease. Breast cancer can be classified into ER (estrogen receptor)-positive and negative subtypes, and HER2 (human epidermal growth factor receptor2)-positive and negative, applying specific biomarkers. Therefore, the growth and spread of cancer of the breast may be significantly impacted by targeting any of these receptors for hormonal substances (8).

Cancer formation in breast is discovered to be primarily driven by estrogen and estrogen receptors. For this reason, women with estrogen-positive breast cancer are frequently treated by blocking the estrogen signalling system by targeting estrogen. In estrogen-based cancers of breast, Selective Estrogen Receptor Modulators, or SERM, have been used to impede tumour development. Tamoxifen was the first medication licensed for estrogen-positive metastatic breast cancer, and it reduced recurrences by around 40% to 50% (9-10).

2. MATERIALS AND METHODS

2.1 Molecular docking

Molecular docking studies performed using the Schrödinger Maestro software version to examine the interactions between newly designed quinoxaline derivatives and the Estrogen receptor (PDB ID: 6WOK, respectively). The study also examined the interactions of the standard drug Tamoxifen with the same receptor.

Estrogen and progesterone alerting are the main routes seen in both regular and malignant breast cells (11-12). The surplus of the steroid hormones progesterone and oestradiol regulates these pathways and can additionally activate the PGR and ER, respectively [13–17]. As a consequence, the majority of medications proposed to treat breast carcinoma work to prevent progesterone and estrogen from attaching to their receptors. ER is therefore regarded as one of the target proteins in the current investigation.

PDB IDs 6WOK was used to get the co-crystallized 3D structure for ER (Figure 1) from the RCSB-Protein Data Bank (PDB). GLIDE was used to obtain Chain A of the structure for the molecule-specific docking research. Polar hydrogen atoms were also inserted after the water-based molecules were eliminated from the basic data on structural. Because docking in GLIDE requires input files in a certain format, the PDB was converted.

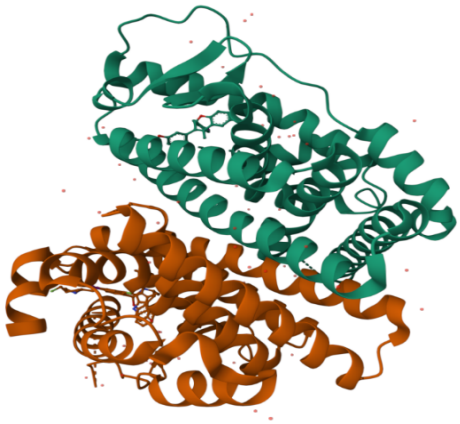

Fig. 1. The complex crystal forms of the estrogen receptor alpha and degrader 6

The Protein Preparation Wizard was used to prepare these structures for the docking investigation. For the purpose of creating a clean and appropriate environment for the docking simulations, the preparation steps involved adding hydrogen atoms and eliminating solvent molecules. In cases where the protein structures had bound ligands, additional steps were taken to ensure accurate simulation of ligand binding interactions and assessment of binding affinities. The protein-ligand complexes were minimized to ensure that the bound ligands were in energetically favourable conformations within the protein binding site. Molecular docking was produced by referencing the cocrystallized bound ligands. These grids helped define the potential binding sites within the catalytic sites of the target proteins (Estrogen receptor), which was crucial for guiding the docking simulations.

As a part of the validation process for the docking protocol, Erlotinib was redocked into the catalytic sites of the proteins. The successful occupation of the similar binding pockets by these reference ligands as seen in the crystallographic structures further supports the accuracy of the docking methodology.

The molecular docking simulations employed the Glide extra-precision (XP) mode, which is known for its high accuracy in predicting ligand binding poses and affinities. The docking process involved compounds 1-8, as well as Tamoxifen. For each molecule, the docking simulations generated and saved three potential binding poses, utilizing the XP mode. This approach allowed for the exploration of different orientations and conformations of the ligands within the binding sites, helping to identify the most energetically favourable binding modes. It has been shown that this approach is helpful in anticipating how small molecule inhibitors will bind to their target

proteins (18). The ligand design strategy is illustrated in Figure 2.

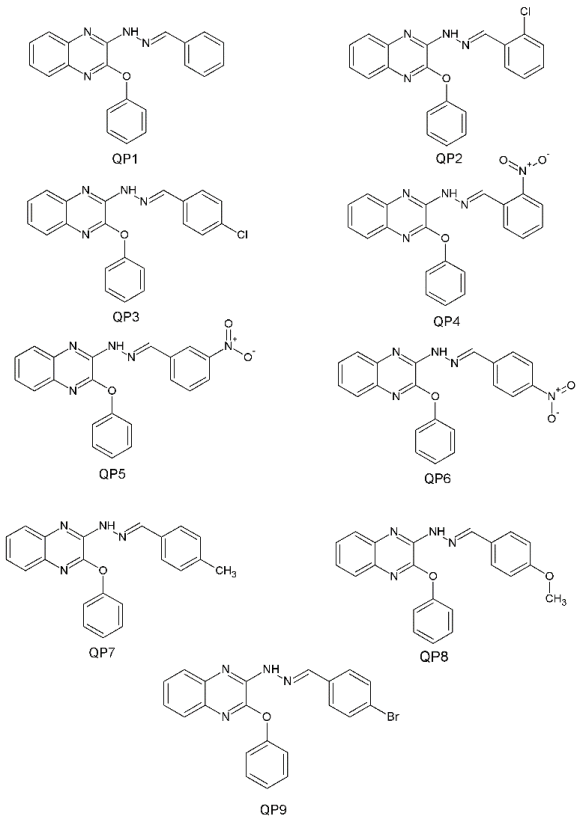

Figure. 2. Designed Phenoxy quinoxaline derivatives (QP1-QP9)

2.2. Drug likeness and synthetic accessibility evaluation

The drug-likeness and synthetic accessibility of the designed compounds were evaluated using the SwissADME web tool. Critical physicochemical parameters such as molecular weight, number of hydrogen bond donors and acceptors, and lipophilicity (log P) were determined, all of which were in accordance with Lipinski's rule of five, suggesting favourable oral bioavailability. Additional drug- likeness filters, including Veber's rule, Pan-assay interference compounds (PAINS) alerts, bioavailability scores, and synthetic accessibility indices, were also determined. These parameters collectively provided a multidimensional assessment of the compounds' pharmacokinetic behaviour, structural alert liability, and synthetic feasibility, which supports their potential to be good drug candidates.

SwissADME bioavailability radar gives a quick and easy visual check to see if the compounds have the right properties to be good drugs. The radar involves six key parameters: solubility (log S ≤ 6), saturation (fraction of sp3-hybridized carbons ≥ 0.25), flexibility (≤9 rotatable bonds), size (molecular weight between 150–500 g/mol), polarity [total polar surface area (TPSA) between 20 and 130 Å2], and lipophilicity (XLOGP3 within −0.7 to +5.0). Compounds that fall inside the pink area are likely to have good bioavailability.

Moreover, blood–brain barrier (BBB) permeability and passive gastrointestinal absorption (human intestinal absorption) were determined using the BOILED-Egg model, which leverages a bidimensional representation based on Wildman and Crippen LogP (WLOGP) (computationally predicted lipophilicity value) and TPSA. According to this model, compounds in the yellow region (yolk) are likely to reach the brain, whereas those in the white region are likely to exhibit efficient passive absorption via the gastrointestinal tract (19).

2.3. ADMET study

In this study, the pkCSM web tool was utilized to predict the ADMET profiles of the designed compounds. The pkCSM platform utilizes graph-based structural signatures, which encode atomic distance relationships within compounds, to develop and refine robust predictive models. Detailed pharmacokinetic and toxicity parameters were generated for each compound by using this tool. Key descriptors analysed included intestinal absorption, BBB permeability, central nervous system (CNS) penetration and skin permeation. In addition, physicochemical properties such as TPSA and the number of rotatable bonds were determined to evaluate their influence on drug-likeness and pharmacokinetic performance. The comprehensive *in silico* analysis revealed that most compounds exhibited favourable ADMET characteristics, thereby reinforcing their suitability for further preclinical development (20).

2.4. MD simulations

Molecular dynamics (MD) simulation is profoundly considered a crucial method for comprehending the dynamic nature of the protein–ligand complex. For each complex, a 100-ns MD simulation production run was performed. The MD simulation was conducted using Gromacs 2021.1, in a Linux operating system environment. In particular, before the simulation production run was initiated, a macromolecular system was prepared. Therefore, ligand structure topology was parameterized using the Swiss Param tool, and the protein topology was produced using the CHARMM36 force field. A time step of 2 fs, a constant pressure of 1 atm, and a constant temperature of 300 K were employed throughout the simulation run. Every protein–ligand complex was submerged in a cubic box system, with a minimum distance of 10 Å between the center and the box edge, and the TIP3P water model was used to solve the entire system. Moreover, the entire system was also neutralized by adjusting the required amount of Na+/Cl− ions. The steepest descent algorithm was used to minimize all systems to address the overlap and close

connections between the atoms. Before the MD simulation production phases, each system was equilibrated with NVT (constant number of Particles Volume, and Temperature ensemble) followed by NPT (constant number of Particles, Pressure, and Temperature ensemble) for 5 ns each. Finally, a 100-ns run was executed for the MD trajectory, analysing parameters such as root-mean- square deviation (RMSD) of protein and ligand, root-mean- square fluctuation, and radius of gyration (RoG), which were calculated by using MD simulation. (21-23)

3.RESULTS AND DISCUSSION

3.1 Molecular docking analysis

In silico molecular docking method enhances drug discovery efficiency and decreases the cost and time of experiment. Designed compounds were subjected to molecular docking using Glide-Schrodinger software. The identified protein structure was subjected to quality review and binding site analysis utilizing the PROCHECK and CASTp servers. Almost 90.2% of residues are located in the most preferred regions, depicted in the Ramachandran plot as shown in Figure 3.

Fig 3. The Ramachandran plot for EGFR tyrosine kinase (PDB ID: 6WOK)

The framework 6WOK has several ligands attached to the ligand-binding domain of the human estrogen receptor α (ERα). And one among such ligand is benzopyran which shows a ligand-binding pocket of ERα receptor. Similar scaffolds may function as a co-crystallized probe or a lower-affinity binder alongside the primary degrader compound in 6WOK, although they frequently act as agonists or antagonists in other crystal structures. This benzopyran's 3-hydroxyphenyl portion most likely forms hydrogen bonds (via direct H-bond or water-mediated interactions) with important polar residues in the ligand pocket, such as Glu353 and Arg394. These locations frequently serve as anchors for estrogen-like ligands and phenolic estrogens in ERα. In the ERα binding cavity, the 4-iodophenyl group and the benzopyran core interact with non-polar side chains (such as the Leu, Phe, and Met residues lining the pocket) to provide hydrophobic packing. The ligand in the pocket is stabilized by this kind of aromatic/hydrophobic interaction. The methyl substituent on the benzopyran ring likely contributes to shape complementarity and steric fit, influencing how the ligand fits relative to the receptor's helix 12 dynamics (which helps determine agonist vs antagonist conformation) (24).

The protein 6wok contains both hydrophilic and hydrophobic areas which is shown in Figure. 4. With an overall near-neutral average hydrophobicity of 0.12, the protein's hydrophobicity plot (231 residues) displays alternating hydrophobic and hydrophilic regions. The lack of long, continuous hydrophobic stretches suggests that the protein is probably soluble and does not contain transmembrane helices. Multiple hydrophilic regions indicate surface-exposed segments that could take part in ligand binding or molecular interactions.

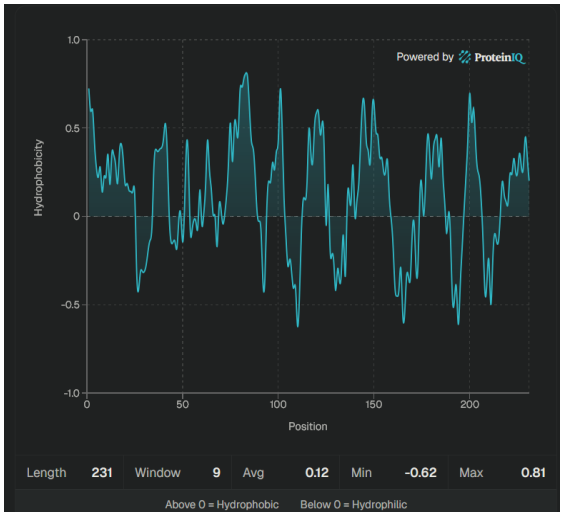

Fig. 4. The hydrophobicity plot distribution of hydrophobic and hydrophilic regions along the protein sequence shown.

3.1.1 Redocking for validation and grid generation

The co-crystallized ligand attached to the protein structure within the binding pocket was removed and subjected to a redocking procedure within the active site. This showed that the important interactions with key amino acid residues of the protein were correctly repeated. The redocking pose of the co- crystallized ligand is depicted in Figure 5. One of the most popular

anticancer medications, tamoxifen is used to treat estrogen receptor α (ERα/ESR1)-positive breast cancer in both early and advanced stages. And it is considered to be the Standard drug in the study. A docking grid was established with x-, y-, and z- coordinates respectively, ensuring coverage of all key amino acid residues within the active site. The grid box dimensions were set to 40Å × 40Å × 40 Å along the respective axes. The above-mentioned dimensions of the grid box were considered while preparing the configuration file for molecular docking.

Compound	Binding affinity	Hydrogen bonding	π-stacking
QP1	−10.872	-	TYR36,55
QP2	−10.415	TYR 36	HIE 91, TYR 55
QP3	−10.327	TYR 87	-
QP4	−9.841	TYR 87, GLN 100	-
QP5	−8.480	TYR 87, GLN 100	PHE 98
QP6	−10.430	SER 9, GLN 100	-
QP7	−10.138	GLY 99	PHE 98, TYR 87
QP8	−10.872	-	-
QP9	−10.974	GLN 89	-
Tamoxifen	**-9.126**		TYR 87

Table 1. The binding affinities and corresponding interaction profiles of selected compounds and the standard drug Tamoxifen

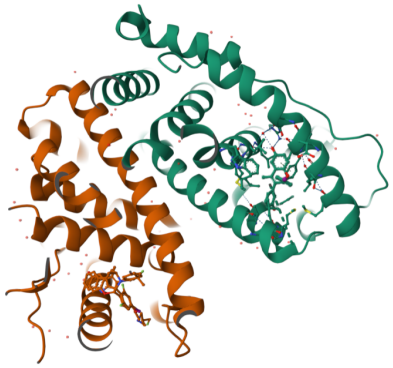

Fig. 5. Redocking pose of the co- crystallized ligand

3.1.2 Post-docking analysis

The resulting docking poses were carefully examined, and those illustrating the most favourable ligand–receptor interactions were selected for further analysis. Among the designed series, most of the QP series compounds exhibited the highest binding affinities against the target protein. Similarly, the standard drug Tamoxifen also shows better results with the same protein. Each selected compound underwent a detailed interaction analysis using the PLIP web server and PyMOL molecular visualization software, and the results were compared with the co-crystallized ligand. The binding affinities and corresponding interaction profiles of these compounds and the standard drug Tamoxifen are summarized in Table 1.

The top selected compounds exhibited significant hydrogen bonding interactions with TYR 36, 87, GLN 100, SER 9, GLY 99 and GLN 89 and hydrophobic interaction with TYR 36, 55, 87, HIE 91 and PHE 98. The co-crystallized ligand exhibited hydrogen bonding interactions with MET 769 and CYS 773. The interactions of all the designed compounds and the Standard drug Tamoxifen with the binding site of the receptor are shown in Figure 6 and Figure 7.

3.1 Evaluation of drug-likeness and synthetic accessibility

Numerous studies have demonstrated that the toxicological profiles and adverse effects of anticancer agents are closely correlated with their molecular weight and inherent chemical characteristics. In light of this, we performed a detailed study of pharmacokinetic parameters and important characteristics relevant to the designed derivatives, utilizing the SwissADME web server to determine chemical characteristics and ADME profiles. The results are depicted in Table 2. The selected compounds and standard drug Tamoxifen satisfied Lipinski's rule of five. In addition, their predicted oral bioavailability was considered moderate, with an Abbott bioavailability score of 0.55. From a medicinal chemistry viewpoint, the compounds did not trigger alerts for PAINS filters. The synthetic accessibility scores of the compounds, ranged from 3 to 5, indicating moderate synthetic feasibility. While synthesis may require careful planning, it remains practical and acceptable for early-stage drug development. Overall, the compounds demonstrated favourable druggability, meeting Lipinski's rule of five, showing promising oral absorptivity, and demonstrating synthetic accessibility. These factors

demonstrate their potential as chemotherapeutic agents or drug leads (25).

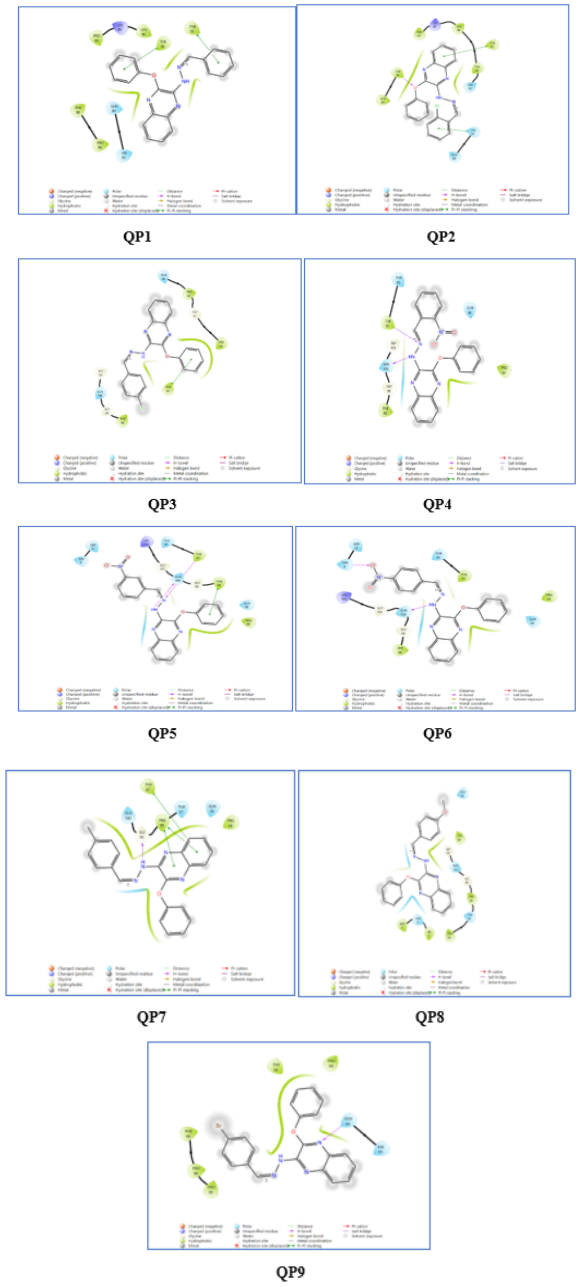

Fig. 6. The interactions between the designed compounds with the binding site of the receptor

Fig. 7. The docking interaction of Standard drug Tamoxifen with the receptor

3.2 ADMET study

The ADMET profiles of the designed compounds were comprehensively evaluated to determine their viability as prospective therapeutic agents, with the corresponding data compiled in Table 3. All compounds demonstrated high predicted gastrointestinal absorption, indicative of efficient oral uptake, while concurrently exhibiting limited potential for CNS distribution. In the context of BBB permeability, a Log PS (permeability-surface area product) which is generally indicative of significant CNS penetration. As CYP enzymes are implicated in the biotransformation of approximately 50% of clinically used drugs, their inhibition can lead to adverse drug–drug interactions and altered pharmacokinetics. All the compounds are showing inhibitory action with CYP1A2, CYP2C19, CYP2C9, CYP2D6 and CYP3A4 indicating a potential for drug–drug interactions. However, this metabolic profile aligns with Erlotinib, a clinically approved EGFR-tyrosine kinase inhibitor, suggesting that the interaction risk is acceptable manageable in the drug development context. Nevertheless, the observed CYP450 inhibition highlights the need for further investigation during later development stages to assess and mitigate potential drug–drug interaction risks (26).

In addition to the core pharmacokinetic advantages, compound QP1 and QP8 was further assessed using advanced drug-likeness metrics provided by SwissADME. The bioavailability radar (Figure. 8 and 9) confirmed that QP1 and QP8 aligns well with the optimal physicochemical space for oral drug candidates in terms of lipophilicity, molecular size, polarity, solubility, and flexibility; however, a deviation in the saturation parameter was noted, reflecting a reduced fraction of sp3-hybridized carbons compared to the ideal threshold.

Furthermore, the compounds were evaluated using the BOILED-Egg model (Figure. 10 and 11), where it was located within the white region of the WLOGP versus TPSA plot. This region is associated with a high probability of passive gastrointestinal absorption, suggesting effective oral uptake. Such a positioning reflects a well-balanced lipophilic–polar profile, a crucial factor in membrane permeability, and reinforces the compound's suitability for oral administration and systemic bioavailability.

Similarly, the compounds were studied for their target prediction and the figure. 12 shows that QP8 has a wide range of targets, but it strongly favors kinases and GPCRs, which are well-known targets for cancer treatments. The existence of several secondary target classes points to possible polypharmacological behaviour, which could improve therapeutic efficacy but also calls for additional in vitro and in vivo testing to assess toxicity and selectivity. This target distribution validates QP8's

biological significance and drug-likeness, supporting its continued study as a viable anticancer candidate.

Compounds	QP1	QP2	QP3	QP4	QP5	QP6	QP7	QP8	QP9	TAMOXIFEN
Molecular weight(g/mol)	340.38	374.82	374.82	385.38	385.38	385.38	354.40	370.40	419.27	371.51
Hydrogen bond donors	1	1	1	1	1	1	1	1	1	0
Hydrogen bond acceptors	4	4	4	6	6	6	4	5	4	2
LogP	3.61	4.09	4.09	3.50	3.50	3.50	3.83	3.28	4.20	5.10
TPSA	59.40	59.40	59.40	105.22	105.22	105.22	108.50	68.63	59.40	12.47
Rotatable bonds	5	5	5	6	6	6	5	6	5	8
Lipinski's rule of five violations	0	0	0	0	0	0	0	0	0	0
Veber's rule violations	0	0	0	0	0	0	0	0	0	0
Synthetic accessibility	3.42	3.42	3.39	3.55	3.53	3.48	3.51	3.56	3.41	3.01
Bioavailability score	0.55	0.55	0.55	0.55	0.55	0.55	0.55	0.55	0.55	0.55

Table 2. Drug-likeness and synthetic accessibility assessment of selected compounds

Compounds	QP1	QP2	QP3	QP4	QP5	QP6	QP7	QP8	QP9	TAMOXIFEN
GI absorption	High	High	High	High	High	High	High	High	High	High
BBB permeation	Yes	Yes	Yes	No	No	No	Yes	Yes	Yes	Yes
P-gp substrate	No	No	No	No	No	No	No	No	No	No
CYP1A2 inhibitor	Yes	Yes	Yes	Yes	Yes	Yes	Yes	Yes	Yes	Yes
CYP2C19 inhibitor	Yes	Yes	Yes	Yes	Yes	Yes	Yes	Yes	Yes	Yes
CYP2C9 inhibitor	Yes	Yes	Yes	Yes	Yes	Yes	Yes	Yes	Yes	Yes
CYP2D6 inhibitor	Yes	Yes	Yes	No	No	No	Yes	Yes	Yes	Yes
CYP3A4 inhibitor	No	No	No	No	No	No	Yes	Yes	No	Yes
Log K_p (Skin permeation cm/s)	-4.81	-4.57	-4.57	-5.21	-5.21	-5.21	-4.64	-5.02	-4.80	-3.50

Table 3. Predicted ADMET parameters of selected compounds

3.3.MD simulation

MD simulation is a powerful computational technique extensively used to explore the dynamic and structural properties of protein–ligand complexes. Due to its excellent profile, QP8 was selected for in-depth investigation using MD simulation. A 100-ns simulation was conducted to evaluate the stability and interaction dynamics of the compound QP8-Estrogen receptor complex. Key parameters, such as RMSD, RMSF, intermolecular hydrogen bonds, Ligand-protein contacts and Ligand torsion profiles, were extracted from the simulation trajectories.

3.1.1 RMSD profile analysis

To assess the conformational and binding stability of the protein–ligand complexes, the RMSD of the protein backbone was calculated from the MD simulation trajectory. Higher backbone RMSD typically reflects conformational rearrangements, whereas lower values suggest greater structural stability. A stable RMSD profile with minimal fluctuations indicates system equilibration. In this study, RMSD for complexes with QP8 and the co-crystallized ligand was calculated and is shown in Figure 13. The average RMSD values for the co-crystal ligand, with both systems displaying consistent trajectories

Ligand RMSD was also analysed to evaluate the positional stability of the ligands during the simulation (Figure. 10). The difference between maximum and minimum RMSD For the co-crystal ligand, indicating limited deviation from their initial binding poses. These findings indicate that both ligands maintained stable

binding within the EGFR-tyrosine kinase active site throughout the simulation

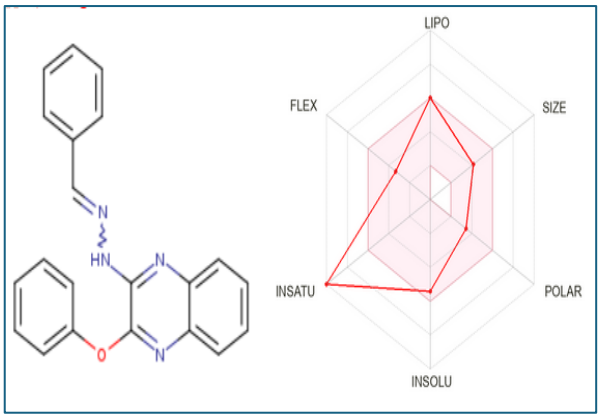

Figure.8. Bioavailability radar for QP1 showing physicochemical behaviour

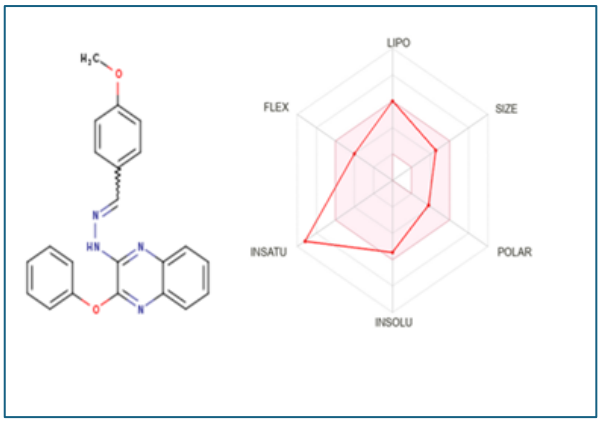

Figure.9. Bioavailability radar for QP8 showing physicochemical behaviour

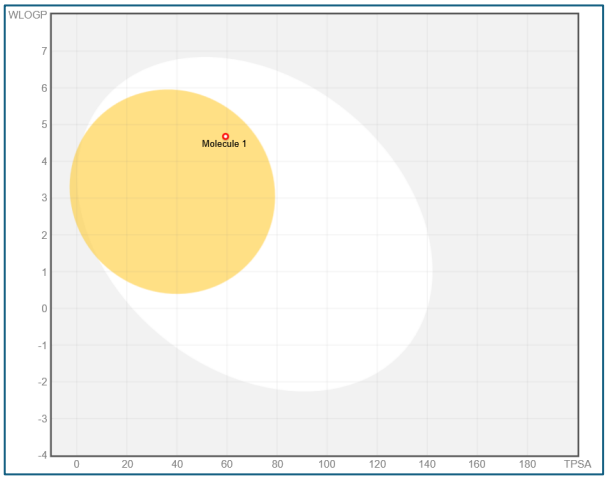

Figure.10. Boiled egg representations for QP1 showing physicochemical behaviour

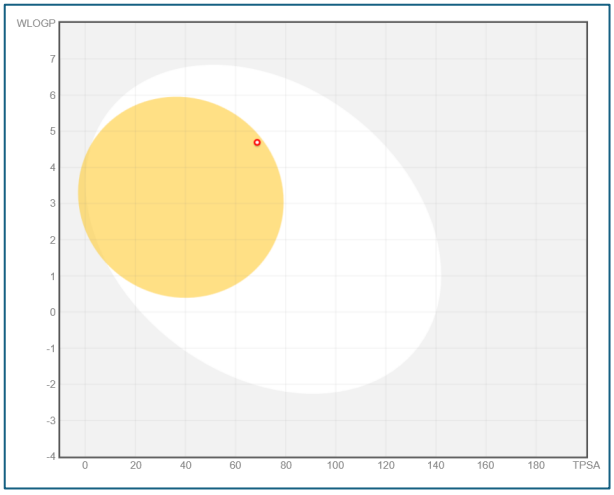

Figure.11. Boiled egg representations for QP8 showing physicochemical behaviour

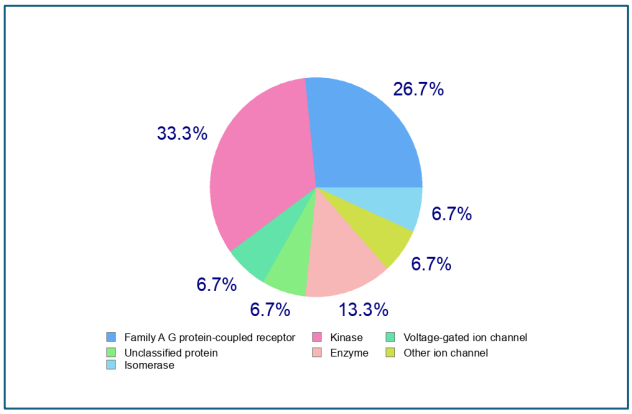

Figure.12. The predicted target proteins for the designed compound QP8 using SWISS ADME

3.1.1 Root-mean-square fluctuation

The RMSF, a key parameter for assessing the flexibility of individual amino acid residues, was systematically calculated for both complexes. These analyses offer valuable insight into the residue-level dynamics of Estrogen receptor. Notably, while the catalytic region remained stable, certain residues exhibited higher fluctuations, reflecting the balance between structural rigidity and flexibility in the presence of QP8 (Figure. 14).

According to the RMSF analysis, the protein permits localized flexibility in loop and terminal regions while maintaining a stable and rigid core throughout the simulation. The protein's favourable dynamic behaviour in the presence of the ligand is suggested by this equilibrium between stability and flexibility, which

supports the accuracy of the molecular dynamics simulation results.

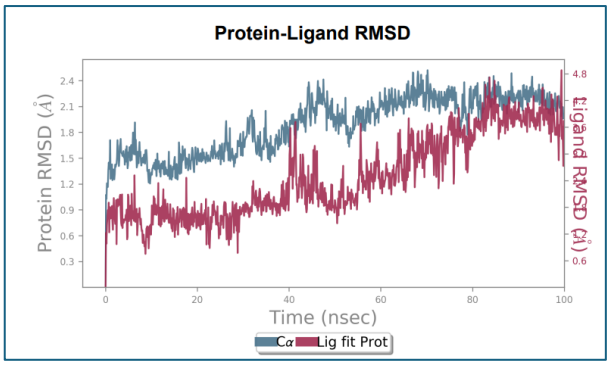

Figure. 13. RMSD plot of the compound QP8

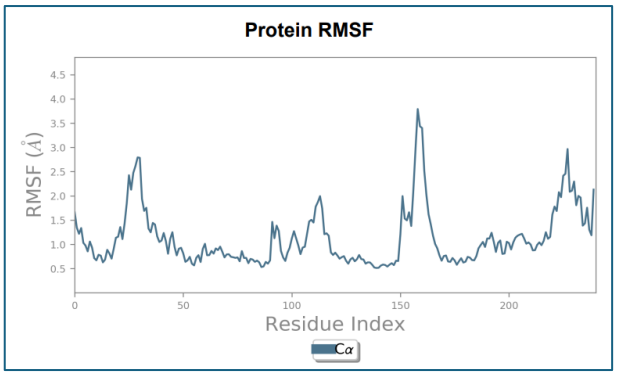

Figure. 14. RMSF plot of the compound QP8

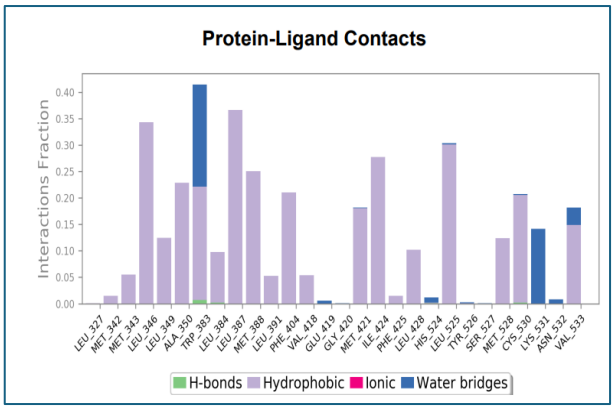

Figure. 15. Protein -ligand contact for QP8

As determined by the interaction profile, the ligand binds to the active site steadily and reliably, mostly through hydrophobic interactions that are augmented by water bridges which is shown in Figure 15. Low nonspecific electrostatic binding, which may promote selectivity, is suggested by the lack of strong ionic interactions.

DISCUSSION

In an effort to assess the anticancer potential of several designed QP derivatives that target estrogen receptor α (ERα), a thorough in silico investigation was conducted in this study. The majority of the designed compounds showed strong binding affinities toward the target protein, sometimes outperforming that of the common medication tamoxifen, according to molecular docking studies conducted using the Glide–Schrödinger platform. The key interactions of the co-crystallized ligand were successfully replicated within the active site, confirming the validity of the docking protocol through redocking.

The designed compounds' favourable binding modes were highlighted by post-docking interaction analysis, which showed that they formed stable interactions with critical amino acid residues through hydrophobic contacts, π-stacking interactions, and hydrogen bonding. Because of its superior binding affinity, ideal interaction profile, and consistency with the binding properties of known ERα ligands, compound QP8 stood out among the series as a promising lead molecule.

All of the selected compounds showed acceptable oral bioavailability, moderate synthetic feasibility, and compliance with Lipinski's and Veber's guidelines, according to drug-likeness and synthetic accessibility assessments conducted using the SwissADME web server. Although possible CYP450 inhibition suggests the need for additional experimental validation at later stages, ADMET predictions further supported their drug-like nature, indicating high gastrointestinal absorption and manageable pharmacokinetic profiles.

The QP8–ERα complex's dynamic stability was better understood by molecular dynamics simulations conducted over a 100 ns duration. A stable protein–ligand complex with few structural aberrations and localized flexibility restricted mostly to loop and terminal regions was validated by the RMSD and RMSF studies. The durability of the QP8 association within the receptor binding pocket was reinforced by protein–ligand contact analysis, which showed that hydrophobic interactions, complemented by water-mediated contacts, primarily controlled the binding stability.

The derivatives of phenoxy quinoxaline have been shown to have estrogen receptor antagonistic action, and they may serve as a well-defined scaffold for upcoming breast cancer research.

CONCLUSION

The proposed phenoxy quinoxaline (QP) compounds showed promising anticancer potential against estrogen receptor α, according to the in-silico evaluation. Reliable binding inside the ERα active site was established by molecular docking investigations, with a number of drugs exhibiting higher affinities than tamoxifen. Due to its

excellent binding profile, attractive drug-likeness, and stable interactions with important residues, QP8 stood up as the most promising lead among them. Further evidence for QP8's stability, bioavailability, and pharmacokinetic appropriateness came from ADMET and molecular dynamics investigations. These results indicate that phenoxy quinoxaline derivatives—especially QP8—represent a promising framework for additional experimental development as ERα-targeted breast cancer treatments.

FINANCIAL ASSISTANCE
NIL

CONFLICTS OF INTEREST
The authors report no financial or any other conflicts of interest in this work.

ETHICAL APPROVALS
This study does not involve experiments on animals or human subjects.

DECLARATION REGARDING USE OF AI TOOLS
The authors declare that artificial intelligence–based tools, including Quill Bot, were used solely for paraphrasing and language refinement of selected sentences and for formatting references in the correct journal-prescribed style. The scientific content, study design, data analysis, interpretations, and conclusions are entirely the original work of the authors. The use of AI tools did not influence the originality of the research or the validity of the results. All authors take full responsibility for the integrity, accuracy, and authenticity of the manuscript.

REFERENCES

1. National Breast Cancer Foundation, Breast Cancer Facts & Statistics, https://www.nationalbreastcancer.org/breast-cancer-facts/ (2026).
2. Abcam, Innovations and Insights in Breast Cancer Research: 2025 Update, https://www.abcam.com/en-us/stories/articles/innovations-and-insights-in-breast-cancer-research-2025-update (2026).
3. National Breast Cancer Foundation: Breast Cancer Facts, https://www.nationalbreastcancer.org/breast-cancer-facts/ (2026).
4. SEER Cancer Statistics: Breast Cancer Facts, https://seer.cancer.gov/statfacts/html/breast.html (2026).
5. BreastCancer.org: Breast Cancer Facts & Statistics, https://www.breastcancer.org/facts-statistics (2026).
6. Nature Medicine, Breast cancer research article (s41591-025-03502-3), https://www.nature.com/articles/s41591-025-03502-3 (2026).
7. World Health Organization, Breast cancer fact sheet, https://www.who.int/news-room/fact-sheets/detail/breast-cancer (2026)
8. Singh A, Mishra R, Mazumder A. Breast cancer and its therapeutic targets: A comprehensive review. Chemical Biology & Drug Design. 2024;103(1): e14384.
9. Den Hollander P, Savage MI, Brown PH. Targeted therapy for breast cancer prevention. Frontiers in Oncology. 2013; 3:250.
10. Masoud V, Pagès G. Targeted therapies in breast cancer: New challenges to fight against resistance. World Journal of Clinical Oncology. 2017;8(2):120.
11. S. Mani, G. Swargiary, S. Gulati, S. Gupta, and D. Jindal, *Mater. Today Proc.*, 80, 2378 (2023).
12. Protein Data Bank Europe, PDB ID: 6WOK, *PDBe*, EMBL-EBI (2020).
13. H. N. Hilton, C. L. Clarke, and J. D. Graham, *Mol. Cell. Endocrinol.*, 466, 2 (2018).
14. A. M. Fowler and E. T. Alarid, *Breast Cancer Res.*, 9, 305 (2007).
15. M. Xue, K. Zhang, K. Mu, J. Xu, H. Yang, Y. Liu, et al., *Oncogenesis*, 8, 32 (2019).
16. S. López-Tarruella and R. Schiff, *Clin. Cancer Res.*, 13, 6921 (2007).
17. T. McFall, B. McKnight, R. Rosati, S. Kim, Y. Huang, N. Viola-Villegas, et al., *J. Biol. Chem.*, 293, 1163 (2018).
18. J. Chem. Inf. Model., 47, 1599 (2007).
19. K. Saritha, M. Alivelu, and M. Mohammad, *In Silico Pharmacol.*, 12, 67 (2024).
20. D. E. V. Pires, T. L. Blundell, and D. B. Ascher, *J. Med. Chem.*, 58, 4066 (2015).
21. K. Kato, T. Nakayoshi, E. Kurimoto, and A. Oda, *Chem. Phys. Lett.*, 781, 139022 (2021).
22. T. Tuccinardi, *Expert Opin. Drug Discov.*, 16, 1233 (2021).
23. Carter and P. Tadi, *StatPearls*, StatPearls Publishing, Treasure Island (FL) (2025).
24. J. R. Kiefer, M. Vinogradova, J. Liang, B. Zhang, X. Wang, and S. Labadie, *Protein Data Bank*, 6WOK (Crystal structure of estrogen receptor α in complex with receptor degrader 6) (2020)
25. A. Mohamed Sheik Tharik and S. N. Meyyanathan, *J. Xi'an Shiyou Univ., Nat. Sci. Ed.*, **17**, 142–169.
26. B. Bakchi, A. D. Krishna, E. Sreecharan, V. B. J. Ganesh, M. Niharika, S. Maharshi, S. B. Puttagunta, D. K. Sigalapalli, R. R. Bhandare and A. B. Shaik, *J. Mol. Struct.*, **1259**, 132712 (2022)
27. K. Kato, T. Nakayoshi, E. Kurimoto and A. Oda, *Chem. Phys. Lett.*, **781**, 139022 (2021).